http://dx.doi.org/10.5665/sleep.3768

Tongue Fat Infiltration in Obese Versus Lean Zucker Rats

Michael J. Brennick, PhD[1,2]; James Delikatny, PhD[3]; Allan I. Pack, MBChB, PhD[1,2]; Stephen Pickup, PhD[3]; Sarika Shinde, BA[1]; Jing-Xu Zhu, PhD[1]; Ivana Roscoe, BS[1]; David Y. Kim, BA[1]; Laurence U. Buxbaum, MD, PhD[4,5]; Jacqueline R. Cater, PhD[6]; Richard J. Schwab, MD[1,2]

[1]Center for Sleep and Circadian Neurobiology, [2]Division of Sleep Medicine, [3]Department of Radiology, [4]Philadephia Research and Education Foundation, Philadelphia, PA, and [5]Division of Infectious Disease, Perelman School of Medicine, University of Pennsylvania, Philadelphia, PA; [6]Biomedical Statistical Consulting, Maple Shade, NJ

Study Objectives: Obesity is the most important risk factor for obstructive sleep apnea (OSA), and the effects of obesity may be mediated by tongue fat. Our objective was to examine the effects of obesity on upper airway structures in obese (OBZ) and non-obese (NBZ) Zucker rats.
Design: Animal study.
Setting: Academic Medical Center.
Participants: OBZ (638.2 ± 39 g; 14.9 ± 1.1 w) and age-matched NBZ Zucker (442.6 ± 37 g, 15.1 ± 1.5 w) rats.
Interventions: Tongue fat and volume and were assessed using: *in vivo* magnetic resonance spectroscopy (MRS), magnetic resonance imaging including Dixon imaging for tongue fat volume, *ex vivo* biochemistry (fat quantification; triglyceride (mg)/tissue (g), and histology (Oil Red O stain).
Measurements and Results: MRS: overall OBZ tongue fat/water ratio was 2.9 times greater than NBZ ($P < 0.002$) with the anterior OBZ tongue up to 3.3 times greater than NBZ ($P < 0.002$). Biochemistry: Triglyceride (TG) in the tongue was 4.4 times greater in OBZ versus NBZ ($P < 0.0006$). TG was greater in OBZ tongue (3.57 ± 1.7 mg/g) than OBZ masseter muscle (0.28 ± 0.1; $P < 0.0001$) but tongue and masseter TG were not different in NBZ rats (0.82 ± 0.3 versus 0.28 ± 0.1 mg/g, $P = 0.67$). Dixon fat volume was significantly increased in OBZ (56 ± 15 mm^3) versus NBZ (34 ± 5 mm^3, $P < 0.004$). Histology demonstrated a greater degree of intracellular muscle fat and extramuscular fat infiltration in OBZ versus NBZ rats.
Conclusions: Genetically obese rats had a large degree of fat infiltration in the tongue compared to both skeletal muscle and tongue tissues of the non-obese age-matched littermates. The significant fat increase and sequestration in the obese tongue may play a role in altered tongue neuromuscular function, tongue stiffness or metabolic function.
Keywords: Dixon imaging, MRI, obesity, obstructive sleep apnea, spectroscopy, tongue, upper airway, Zucker rats
Citation: Brennick MJ, Delikatny J, Pack AI, Pickup S, Shinde S, Zhu JX, Roscoe I, Kim DY, Buxbaum LU, Cater JR, Schwab RJ. Tongue fat infiltration in obese versus lean Zucker rats. *SLEEP* 2014;37(6):1095-1102.

INTRODUCTION

Obesity has become a national epidemic with more than 66% of US adults considered as overweight (body mass index [BMI] > 25 kg/m^2) and 37.5% are considered obese (BMI > 30 kg/m^2).[1-5] Moreover, obesity is the most important risk factor for obstructive sleep apnea (OSA).[1,6,7] However, we do not understand the mechanism underlying the relationship between obesity and sleep apnea. Obesity is thought to have direct and indirect effects on upper airway structures.[8] Weight gain may increase the size of soft-tissue structures by a variety of mechanisms, including muscle cell hyperplasia or hypertrophy, fat-related collagenous or extracellular increases, or by direct fat deposition within these tissues.[9] An autopsy study[10] demonstrated that the human tongue has a remarkably high percentage of fat and that tongue weight and percentage of tongue fat are related to degree of obesity. Increased tongue size has been shown to be a risk factor for OSA.[11,12] We have recently shown that there is more fat in the tongue of obese patients with sleep apnea than obese controls.[13] Studies have also shown that there is direct fat and inflammatory cell infiltration into the soft palate.[9,14-16] Such studies suggest that fat infiltration into the upper airway soft tissues is important in understanding the relationship between obesity and OSA.

Animal models provide the capability to directly assess the volume of tongue fat. Therefore, the current study was designed to quantify the degree to which obesity is directly related to increased tongue fat using both noninvasive methods such as magnetic resonance spectroscopy (MRS),[17,18] volumetric magnetic resonance imaging (MRI)[12,19] with fat-enhanced imaging,[13,20] and *ex vivo* tissue analyses including biochemical lipid analysis[21] and histological examination.[22] We chose the established Zucker rat genetic model of obesity,[23] wherein the obese genotype (fa/fa) has been found to have a defect in leptin signaling that inhibits or prevents the sensation of satiety. The obese Zucker rats (OBZ) gain a significant amount of weight given ad-lib feeding. The nonobese Zucker rats (NBZ) also gain weight with age, albeit to a lesser degree, but without hyperlipidemia, and obesity-related consequences of the OBZ rats.[23] Thus, the OBZ rats (8 w or older) are substantially heavier than age-matched NBZ rats, and have been shown in our laboratory and others to have upper airway narrowing[24] and increased pharyngeal collapsibility.[25] Thus, this rodent model of obesity exhibits characteristics of obesity-related upper airway compromise.

The goals of this investigation were to compare age-matched Zucker rats using *in vivo* MRS and volumetric MRI of the tongue along with biochemistry and histological analysis of *ex vivo* tissues to determine the effects of obesity on fat in the tongue. We also used the same measurements in the masseter

A commentary on this article appears in this issue on page 1031.

Submitted for publication September, 2013
Submitted in final revised form January, 2014
Accepted for publication February, 2014
Address correspondence to: Richard J. Schwab, MD, Professor, Department of Medicine, Division of Sleep Medicine, Pulmonary, Allergy and Critical Care Division, Co-Director, Penn Sleep Center, University of Pennsylvania Medical Center, 3624 Market Street, Suite 205, Philadelphia, PA 19104; Tel: (215) 349-5477; E-mail: rschwab@mail.med.upenn.edu

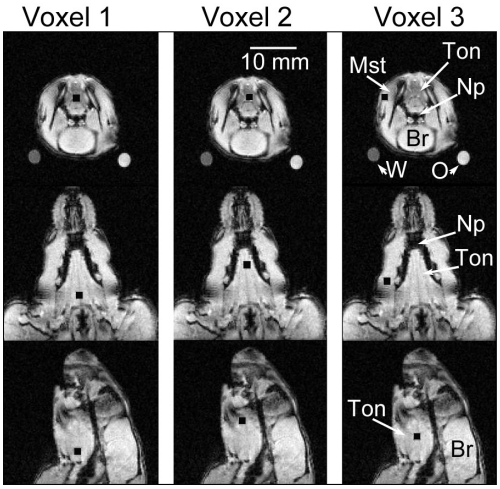

Figure 1—Location of voxels in representative obese Zucker rat. The exact location of three voxels (black squares) that were studied using the spectroscopy protocol in nine magnetic resonance imaging (MRI) slices from a single obese rat are shown. The first column shows the location of the first magnetic resonance spectroscopy (MRS) tongue voxel (Voxel 1) in the axial, coronal, and sagittal views (rows labeled, far right); the second column shows the location of the second tongue voxel (Voxel 2); and the third column shows the location of the masseter muscle voxel (Voxel 3). The posterior tongue voxel was placed proximal to the hyoid bone. The second (anterior) tongue voxel was placed 2-4 mm anterior to the posterior voxel in the middle part of the tongue. The third voxel was placed in the masseter muscle, lateral to the mandible bone. Annotations on the third column of images show: Mst, masseter muscle; Ton, tongue; Np, nasopharyngeal airway; Br, brain. Calibration bar (second column) = 10 mm and applies to all images. In the top row the oil (marked "O") and water phantom (marked "W") show the cross section of the tubular glass phantoms as round dots outside the rat but within the images. These phantoms were used to calibrate the Dixon method for analysis of fat content in the Dixon spin-echo magnetic resonance images (images shown above are T1 weighted, scout images not Dixon protocol images; see supplemental material for details on the imaging protocols and analyses).

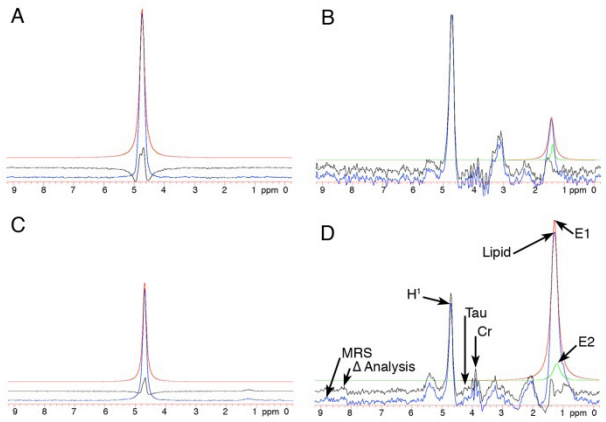

Figure 2—MR H^1 spectra of tongue muscle in non-obese Zucker (NBZ) and obese Zucker (OBZ) rats. The H^1 spectra obtained during nonwater suppressed acquisition, in panels **A** (NBZ) and **C** (OBZ) show a single spectral peak at 4.7 ppm, that is the resonant frequency of water for the 200 MHz imaging system in this experiment. The water-suppressed point-resolved multiecho spectroscopy (PRESS) acquisition H^1 spectra in panels B (NBZ) and D (OBZ) are, respectively, from the same tongue voxels from which the nonsuppressed water spectra **(A,C)** were obtained. Color-coded curves are used in the figures to differentiate the original spectral data (blue lines) from the computer-generated curve-fitted data in each panel. The red lines denote the estimated area under the water spectra and lipid peaks **(A,C)**, whereas in **B** and **D** two polynomial equations were combined (red and green lines) to better estimate the area under the lipid peak. The black lines represent the difference in calculated area from the original (blue line) data. In panel **D**: MRS, the blue line original spectra; Δ analysis, the black line as described above; typical spectral peaks (Tau, taurine; CR, creatinine). H^1 denotes the water peak; Lipid denotes the lipid peak; and E1 and E2 are peaks of the computer-generated curves that combine to estimate the lipid peak.

muscle as a control (a representative other upper airway muscle). We hypothesized that: (1) fat infiltration would be greater in the tongue of OBZ rats than in age-matched NBZ rats; (2) given what has been demonstrated in humans,[10] there would be a distinct topography to the fat deposition in the tongue with more fat at the tongue base; and (3) obesity-related fat infiltration would be comparatively greater in the tongue than in other upper airway muscles in the OBZ rats and of upper airway muscles in NBZ rats. Part of this investigation has been presented in abstract form.[26,27]

METHODS

This study was approved by the Institutional Animal Care and Use Committee (IACUC) of the University of Pennsylvania. OBZ and NBZ (male only) rats were studied in age-matched groups for each of four study components: (1) MRS of the tongue and masseter muscle in OBZ and NBZ rats; (2) MRI of OBZ and NBZ rats with a Dixon spin-echo fat-weighted protocol for analysis of tongue fat and tongue volume; (3) biochemical analysis[21] of triglyceride (lipid) content of post-mortem tongue and masseter muscles in OBZ and NBZ rats; and (4) histological analysis of representative tongue sample tissues of OBZ and NBZ rats. See the supplemental material for additional details for each measurement.

MRS and Imaging: General

H^1 spectra for MRS and MRI were obtained in a 4.7 T MRI system (Agilent, Palo Alto, CA) equipped with a Litz® volume coil (Doty Scientific, Columbia, SC) in anesthetized, spontaneously breathing rats. Single voxel H^1 magnetic resonance spectra in each rat were acquired in three voxels (2 × 2 × 2 mm) using the point-resolved multiecho spectroscopy (PRESS) sequence[17] with water suppression followed by scanning with no water suppression. Figure 1 shows the placement of the three voxels in a representative OBZ rat from T2-weighted scout images. MRS data were processed using Mac Nuts® (Acorn NMR INC., Livermore, CA) software. The lipid peak was assumed to be at 1.3 ppm in the adjusted spectrum, where the center of the water peak was set to 4.7 ppm that is the known standard for this 4.7T, 200 MHz system[17] (Figure 2). The lipid content was determined by taking the ratio of area of the lipid peak in water-suppressed spectra, to the area of the water peak of the same voxel from the spectra acquired without water suppression.[17]

Tongue Volume and Tongue Fat by MRI

On the same day or within 2-3 days subsequent to the MRS experiment, a Dixon three-point protocol,[20] series of

Table 1—MRS results (± SD)

			Fat/water ratio (± SD)			
	Weight (g)	Age (w)	Tongue posterior	Tongue anterior	Tongue average	Masseter muscle
NBZ (n = 13)	437.9 ± 35.4	15.3 ± 1.5	1.7 ± 1.7	2.0 ± 1.1	1.9 ± 1.1	0.35 ± 0.42 (n = 4)
OBZ (n = 11)	639.4 ± 46.7	15.3 ± 1.3	4.5 ± 3.0	6.5 ± 4.5	5.5 ± 2.9	1.15 ± 0.61 (n = 6)
P value	0.001	0.95	0.072	0.002	0.002	0.038 *

P values from analysis of variance except * from two-tailed *t*-test. The number of successful spectra for the masseter muscle was lower secondary to decreased signal-to-noise ratio. MRS, magnetic resonance spectroscopy; NBZ, non-obese Zucker rats; OBZ, obese Zucker rats; SD, standard deviation.

spin-echo images were used to obtain 13, 2.0-mm-thick axial slices that encompassed the tongue in the rat upper airway. Briefly, the Dixon protocol MRI provided both high-contrast proton-weighted images and fat-weighted images from two sets of anatomically identical slices. Manual segmentation and a threshold method were combined using computer overlay (Amira®, VSG, Burlington, MA) to determine the tongue volume and tongue fat in OBZ and NBZ rats.

Biochemical Methods and Analysis

Following the MRS and MRI experiments, the rats were euthanized by CO_2 insufflation. The tongue was surgically removed by cutting the ventral mucosal tissues in the oral sulcus adjacent to the tongue followed by bilateral section of the mandible at the temporal bony attachment. Approximately 0.5 g of tongue tissue and masseter muscle tissue was used for biochemical analysis. The Folch method for lipid purification combined with enzymatic colorimetry was used to assess triglyceride content of the tongue and masseter muscles.[21,28]

Histological Methods

The histology protocol was designed to examine fat distribution in the OBZ and NBZ rat tongues. i.e., homogenous or regional distribution, and reveal the degree of fat infiltration within or outside muscle cells. Oil Red O staining[22,29] was used with hematoxylin counterstain. Two OBZ and NBZ rat tongues were used for histological analysis.

Statistical Methods

A mixed-model analysis of variance ANOVA was used on each submethod section, i.e., MRS, biochemistry, and MRI analyses.[30] In all cases, for main effects and Tukey adjusted *post hoc* contrasts, significance was assumed at $P < 0.05$.[31]

RESULTS

The number of rats (OBZ and NBZ) used in each substudy is described in Tables 1 through 3, as is their weight and age. Overall, differences in age between OBZ and NBZ rats studied in each group were negligible, whereas OBZ body weight was approximately 30% greater than in NBZ rats at the average study age of approximately 15 w (see Tables 1 and 3). Two of the three quantitative methods to study fat content in the rat tongues were noninvasive (MRS and MRI), whereas the third, invasive method, i.e., biochemical tissue lipid analysis, allowed us to obtain tissue lipid concentrations from direct measurements of tongue and masseter muscle tissues, thus providing a basis for validation of the noninvasive determinations.

MRS Results of Fat-to-Water Ratios in Tongue and Masseter Muscle Tissue Voxels

Figure 1 shows the exact location of voxels (black squares) that were studied with spectroscopy in nine magnetic resonance scout images from a single OBZ rat. In each MRS acquisition we used the same size voxels. Although the loci are shown for a representative (OBZ) rat, these locations could be repeated without difficulty in each animal studied.

The display and analysis of H^1 spectra in similarly located tongue voxels from NBZ and OBZ rats are shown in Figure 2. The lipid peak in D (OBZ rat H^1 spectra with water suppression) is much higher than the lipid peak in B (NBZ rat H^1 spectra with water suppression). The non-suppressed water peaks (A and C) were used to normalize the results from similarly sized voxels in different rats. The MacNuts program integrated the area under the computer-generated curves from polynomial nth order equations. This method allowed a direct comparison of the ratio of the area under the water peak to the area under the lipid peak for each computer-analyzed spectra. In this example (Figure 2) the fat-to-water ratio for OBZ was 1.65 and NBZ was 0.38.

The fat/water ratios presented in Table 1, are quantitative nondimensional normalized values that compare the relative lipid content in voxels in the different animals. Comparisons between rat obesity groups showed a significant increase in OBZ versus NBZ in the anterior region ($P = 0.002$) and a trend toward an increase in OBZ versus NBZ in the posterior region ($P = 0.072$). Overall differences averaged across posterior and anterior tongue regions showed a significant ($P < 0.002$), nearly threefold increase (5.5 ± 2.9 compared to 1.9 ± 1.1), in the fat/water ratio (OBZ > NBZ rats).

Within rat types, comparisons (not shown in Table 1) between tongue average fat/water ratios and the masseter muscle (one-way ANOVA) showed that in NBZ, the tongue fat/water ratio was 4.7 times greater than NBZ masseter muscle ($P < 0.002$), and OBZ tongue fat/water ratio was also significantly (4.8 times) greater than OBZ masseter muscle ($P < 0.0002$). Additionally, as shown in Table 1, OBZ masseter muscle fat/water ratio was more than three times greater than that of NBZ ($P < 0.038$). Thus, from MRS analysis, in both NBZ and OBZ rats, fat was sequestered to a much greater degree in the tongue than in a control upper airway muscle (masseter) and the effect of obesity (comparing OBZ to NBZ rats) caused a similar, proportional increase of the fat/water ratio in both the tongue and masseter muscles. The absolute magnitude of the increase was, however, much greater in the tongue.

Table 2—Tongue volume and fat volume by MRI

	Tissue volume (mm^3 ± SD)			Dixon fat volume (mm^3 ± SD)		
	Posterior	Anterior	Total	Posterior	Anterior	Total
NBZ (n = 7)	559.7 ± 20.5	473.7 ± 23.4	1033.4 ± 18.1	7.8 ± 3.2	26.2 ± 2.8	33.9 ± 5.3
OBZ (n = 7)	595.6 ± 24.5	434.6 ± 64.5	1030.0 ± 61.5	15.2 ± 5.8	40.4 ± 10.9	55.6 ± 15.1
P value	0.47	0.56	1.0	0.57	0.037	0.004

NBZ, non-obese Zucker rats; OBZ, obese Zucker rats; SD, standard deviation.

Table 3—Biochemistry results (± SD)

			Triglyceride/tissue (mg/g ± SD)		
	Weight (g)	Age (w)	Tongue	Masseter	Tongue vs. Masseter
NBZ (n = 8)	450 ± 43	14.5 ± 0.93	0.82 ± 0.26	0.28 ± 0.08	P < 0.67
OBZ (n = 10)	637 ± 31	14.9 ± 0.90	3.57 ± 1.7	0.28 ± 0.11 *	P < 0.0001
P value	0.001	0.46	0.0006	0.94	

P values along bottom row for Tukey adjusted comparisons of NBZ vs. OBZ. P values in last column are Tukey adjusted comparison of tongue and masseter within NBZ or OBZ rat types. A reduced N = 7, denoted by (*) for OBZ masseter group. NBZ, non-obese Zucker rats; OBZ, obese Zucker rats; SD, standard deviation.

MRI Volumetric and Dixon Fat Results

The results for the MRI tongue volumetric analysis and Dixon tongue fat analysis are summarized in Table 2.

The regions (posterior and anterior) refer to portions of the tongue used for MRI analysis in NBZ or OBZ rats (see supplemental material). In each rat group the *a priori* divisions of posterior and anterior tongue region yielded two significantly different regional volumes, such that for NBZ rats, the anterior tongue volume was greater than posterior ($P < 0.004$) and similarly for OBZ anterior tongue volume was greater than posterior ($P < 0.0001$). ANOVA results showed that the interaction between groups: rat type (NBZ and OBZ), and region (anterior, posterior, or total), was marginally significant at $P = 0.06$. However, Tukey adjusted *post hoc* tests showed (bottom row on Table 2) that there was no significant difference in MRI-measured tongue volumes between the NBZ versus OBZ groups for either the anterior or posterior region and that the total tongue volume was not different between NBZ or OBZ rats.

Although there was no major difference between rat groups in tongue volume, total fat volume, using the threshold analysis method on the Dixon fat-discriminated images was significantly greater overall, in the OBZ rat tongues compared with those of the NBZ rats ($P = 0.004$). There was a significant increase in Dixon fat volume in the OBZ anterior region compared to the same region in NBZ rats ($P < 0.037$) but no significant difference in the posterior region between OBZ and NBZ Dixon fat-determined volumes ($P = 0.57$). The results also indicated (not shown in Table 2) that there was a significantly greater fat volume in the anterior region relative to the posterior region for both NBZ ($P < 0.003$) and OBZ ($P < 0.0001$) rat types that was more pronounced for the OBZ rats.

Biochemical Measurement of Tongue Lipids

The biochemical analysis showed significantly greater triglyceride/tissue weight (mg/g) in OBZ rat tongues compared to NBZ rat tongues ($P < 0.0006$) (see Table 3). In contrast to the MRS measurements, there was no significant difference in masseter muscle triglyceride between OBZ and NBZ rats ($P = 0.94$). When tongue and masseter muscle were compared between rat types, in the NBZ rat, triglyceride/tissue was 2.9 times greater in the tongue than in the masseter muscle, although the adjusted P value (Table 3, $P < 0.67$) indicated that this was not a significant increase. However, triglyceride was more than 12.7 times greater in the tongue than masseter muscle in OBZ rats ($P < 0.0001$). Thus, age-matched OBZ rats had significantly more fat in the tongue muscle compared to NBZ rats and, specifically in OBZ rats, there was also a highly significant increase in tongue fat compared to fat in a control skeletal upper airway muscle (masseter).

Histology

The objective of the histology component was to use the fat-specific stain, Oil Red O to identify fat deposits in the tongues of NBZ and OBZ age-matched rats. From this examination a topology on the general degree and distribution of fat infiltration was observed. In Figures 3A and 3B, representative data for a single OBZ rat are shown. On the left side (Figure 3A) is the scout image that was used to obtain the MRS data for that rat, whereas the panel on the right is a sagittal slice stained with Oil Red O and hematoxylin counterstain (provides blue color for cellular membrane identification).

The comparison of NBZ sagittal tongue slices to OBZ slices from comparable locations in Figures 4A-4F provides a basis for several observations. First, there is visibly more fat in the OBZ rat tongue slices that in the NBZ rat tongues. Although a quantitative measure from histological analysis was not performed, a general qualitative examination revealed that there was fat found to a much greater degree in the OBZ tongues slices than in NBZ rat tongue slices. The distribution of fat was heterogeneous in both the NBZ or OBZ rat tongues. There was

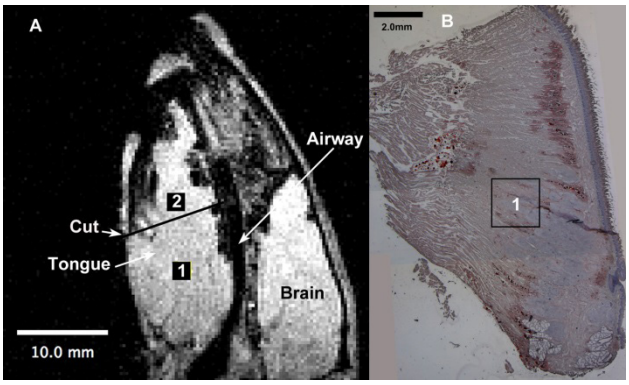

Figure 3—Sagittal magnetic resonance imaging MRI of obese rat tongue compared to postmortem histological slice. Panel A shows the midsagittal image of an obese rat (same rat from which magnetic resonance spectroscopy (MRS) spectra are shown in Figure 2). The rat in both images is oriented with the nose (anterior) toward the top of the image and the posterior tongue and larynx toward the bottom of the frame. In panel **A**, the location of the two voxels (2 × 2 × 2 mm) used for MRS, are drawn to scale, marked, 1 and 2 and highlighted using black squares. These locations depicted on the original scout image were aligned from the scanner data during the MRS protocol. Location 1 is superimposed to scale in the approximate location, on the histological slice in panel **B**. Note that these are thin slices (showing only one face of the three-dimensional voxel) and fat content was dispersed throughout the tissue, not just in the single sagittal slice. On panel **A**, the Cut line denotes the approximate location below which the histological slice in panel **B**, was obtained (the anterior portion of the tongue is not shown in this histology slice). Note that left and right panels have individual but different scale bars; in the lower left (10.0 mm, **A**) and upper right (2.0 mm, **B**).

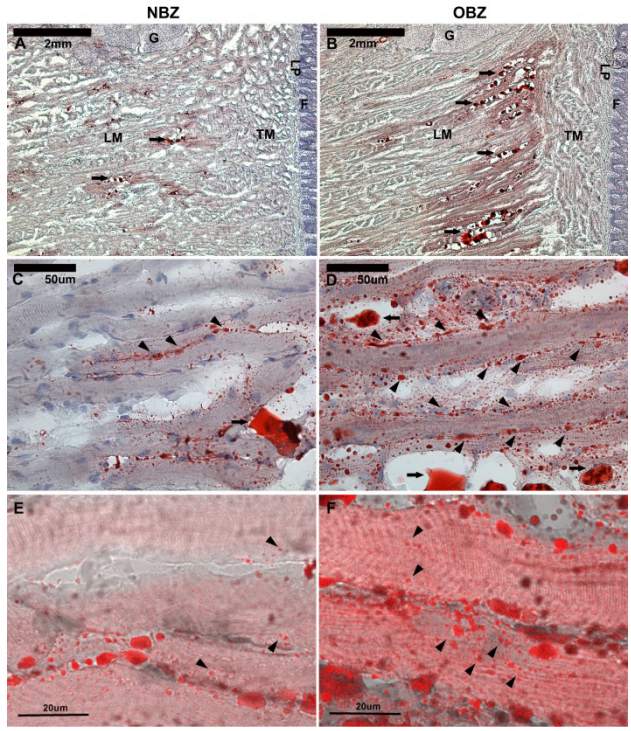

Figure 4—Histological panels **(A-F)** with Oil Red O staining at increasing magnifications (top to bottom). Fat distribution in midsagittal sections of tongue tissue of lean and obese Zucker rats (NBZ and OBZ) is shown. NBZ rats are on the left **(A,C,E)** and OBZ rats are on the right **(B,D,F)**. Neutral lipids are stained red. Hematoxylin counterstain shows cell membranes and organelles in blue. There is much more intracellular and extracellular fat in OBZ slides than NBZ. LM, longitudinal muscle fibers; TM, transverse muscle fibers; G, glands near posterior base of tongue; LP, lamina propria; F, filiform papillae of the dorsal mucosa. In **A** and **B**, calibration bars are 2 mm (40x). Full arrows (with "tails") show neutral lipids accumulated between longitudinal muscle fibers (LM). In panels **C** and **D**, the same region as **A** and **B** are shown in high magnification (400x); calibration bars are 50 μm. Full arrows show large accumulated lipids, and arrowheads show lipid droplets lined on the edge of muscle fibers. Panels **E** and **F** are confocal microscopy images with differential interference contrast image overlay to show intracellular fat. Arrowheads show different sizes of lipid droplets within muscle fibers. Calibration bars are 20 μm.

no particular region (posterior versus anterior, or ventral versus dorsal) where the concentration of fat appeared to be greater than the other. There was fat both inside and outside of muscle cells. There are fat globules or neutral lipids (denoted by full length arrows) that are outside the longitudinal muscle cells in panels C and D. However, arrowheads (no tails) in the same two panels (C and D) show lipid droplets on the edge, apparently inside the longitudinal muscle cells. There is also Oil Red O staining in smaller size spots throughout the muscle cells. Thus, the histology findings are consistent with other published data,[22,29] in that tongue fat can be visualized in both adipose and muscle cells.

Thus, this qualitative histological examination demonstrates that fat is distributed throughout the tongue with relatively more fat in the OBZ rat tongues that in NBZ rat tongues. In addition, this histoanatomic study component provides evidence of intramuscular and extra-muscular (adipose cell) fat deposits and provides evidence of tongue fat infiltration.

DISCUSSION

The goal of this study was to compare the degree of infiltration of fat in the tongue muscle of OBZ and NBZ rats and compare that to differences in another representative upper airway muscle, the masseter. This question is important because obesity is the major risk factor for OSA in adults,[6,7] although the mechanism underlying that is unknown. The major findings of this paper were that (1) there was a large degree of fat infiltration in the tongue muscle in genetically OBZ rats as compared to tongues in NBZ rats and that (2) fat accumulation in the OBZ rat tongues was from 4.8 times (by MRS analyses) to 12.9 times greater (biochemical analyses) than fat measured in another representative upper airway skeletal muscle, i.e., the masseter muscle in the obese rats. The volume of the OBZ rat tongue was not greater than the NBZ rat tongue. However, total fat volume measured by magnetic resonance fat-weighted Dixon image analysis was significantly greater in OBZ rat tongues. This increase in tongue fat was primarily in the anterior region of the OBZ rat tongue compared to that of the NBZ rat tongue (fat in the posterior tongue regions was not different). Because total tongue volume was not altered, tongue fat presumably displaced other tongue tissue components (water, muscle, or components of the extracellular matrix). Importantly, the increase in tongue fat in OBZ rats was demonstrated with several methods, including noninvasive imaging and spectroscopy, and biochemical and

histological examination of dissected tissues; these methods provide consistent results.

We chose to examine age-matched adult male OBZ and NBZ rats in a cross-sectional study because this allowed us to control for age and sex as confounders. The techniques used all led to the same conclusions. There are some limitations with each of our study techniques, which need to be discussed.

Our MRS methods used multiple voxels in order to obtain a sampling of tissues in both the posterior and anterior portions of the tongue. The voxel size was chosen to obtain a spectral acquisition that could be resolved into several H^1 peaks as demonstrated in Figure 3. Pilot testing allowed us to choose a voxel size that could be repeated with the same protocol and provided a good overall signal-to-noise ratio. In the analysis, in some cases, where the lipid peak was complex or composed of two peaks, multiple curve fit approximations were combined to obtain the best fit to area under the lipid peak(s). Use of the curve fit methods allowed us to incorporate the unsuppressed water peak (taken at the same magnetic resonance receiver gain) as a normalizing control, so that the ratio of areas under the lipid peak to the area under the water peak could be used for quantitative comparisons.

Location of the voxels adhered to a protocol that required knowledge of the rat anatomy to set up the MRI acquisition variables. The main difficulty in the MRS protocol was decreased signal (and consequent baseline noise increase) when voxels of the masseter muscle were acquired and analyzed. This problem was difficult to avoid without altering the variables we wanted to keep constant for the purpose of voxel to voxel comparisons. The lower quantity of fat in the masseter muscle, as shown by the results of the biochemical analysis, further lowered the lipid peak in MRS spectra, limiting the usable data to those where signal-to-noise ratio was adequate to analyze. Thus, the difficulty in obtaining data with MRS in the masseter muscle was directly related to the low signal-to-noise ratio.

The Dixon analysis followed methods from similar studies[13,19,20,32] wherein validation for the general techniques are described. We found an overall increase in total tongue fat in OBZ versus NBZ rats using the Dixon approach, and this method also showed that fat accumulation was greater in the anterior region of the tongue of the OBZ rat was greater than in the NBZ rat (Table 2).

The biochemical analysis was performed according to established procedures using the Folch method for lipid separation in biological tissues combined with an enzyme colorimetric method of triglyceride evaluation. This method (detailed in the supplemental material)[21,33] is well established and the specifics of the techniques were customized to separate the free biochemical triglyceride from that in the phospholipid cell wall. Initial testing was repeated on various starting quantities of tissue in order to determine the optimum reagent quantities that would consistently provide concentrations within the standard curve range of the colorimetry step. The overall coefficient of variation of triplicate measures were less than 15% and in most cases the coefficients of variation were less than 10%, indicating repeatability and confidence in the triplicate colorimetric measurements. Additionally, using a single stock quantity of triglyceride standard solution (200 mg/mL) for all trials provided good precision and reliability for the biochemistry protocol.

The histology analysis was designed to provide an in-depth examination of the distribution of fat in the tongue using the Oil-Red-O staining protocol.[22,29] These results provided a clear indication of fat both within and surrounding the tongue muscle cells whereas the increase in overall fat between OBZ and NBZ slices was evident.

Obese and lean phenotypes of both mice and rats have been widely used to examine respiratory mechanics and the effects of obesity.[19,23-25,34-37] Despite differences between rodents and humans, such as the rodent upper airway being rectilinear compared to a more curved human airway, studies in our laboraotry and others [24,25,38,39] have made important observations based on anatomic homology in experiments under controlled conditions not possible in human studies. For instance, we have shown that OBZ rats have a more narrow airway compared to age-matched NBZ rats,[24] whereas Nakano et al.[25] have shown greater collapsibility in the upper airway of OBZ rats. Thus, although the Zucker rat is not a specific model of OSA, it can be used to examine the relationship of obesity to tongue fat accumulation and how tongue fat can affect airway narrowing and collapsibility. Similar relationships between tongue fat and airway size have been shown in New Zealand obese mice.[19]

One of the unexpected findings in this study was that there was no significant difference in tongue volume between age-matched OBZ and NBZ rats. The MRS results, the MRI-Dixon method analysis, the biochemistry, and the histology did show a significant increase in the quantity of fat in the OBZ compared to NBZ tongues. Because the amount of fat we found did not alter the volume of the tongue, presumably the increased fat in OBZ rats displaced components such as muscle tissue, extracellular water, or extracellular matrix components. Although we did not find a simple or direct relationship between tongue fat accumulation and tongue volume change, a within-animal longitudinal study design would provide more information on whether fat accumulation alters tongue tissue volume.

We found by the Dixon image analysis that total fat volume in OBZ rat tongues was significantly greater than in NBZ rat tongues and that the increase in the anterior region in OBZ rat tongues was also significantly greater than the anterior tongue region of NBZ rats. There was no significant difference between OBZ and NBZ rats in the fat volume in the posterior tongue regions. The amount of fat in the posterior region was comparatively lower than in the anterior region. A similar pattern was seen in the MRS results, i.e., an anterior regional fat/water ratio in OBZ rats that was greater than that of NBZ rats whereas no significant difference was found in the posterior fat/water ratios between OBZ and NBZ rats. The greater anterior tongue fat accumulation is an interesting finding considering that other studies have found that muscle fiber type in aged rats tend to shift toward more slowly contracting fibers and this change predominates in the anterior portion of the tongue.[40]

In our histological investigation we found that there was fat infiltration throughout the tongue, in both anterior (midtongue to tip) and posterior (midtongue to base) locations. The fat in rat tongues was not only found from anterior to posterior loci but was found within muscle cells, within connective tissue fascia and within adipose cells. Thus, lipid deposits were distributed in a heterogeneous fashion, anatomically and in different types of regions and cellular compartments.

The cause of obesity in the OBZ rat is believed to involve a deficit in leptin signaling, with a leptin receptor defect at the hypothalamic level.[41] Impaired leptin release or signaling at the adipose cell and within muscle cells may also be altered in the fa/fa OBZ rat.[41] Thus, a defect in leptin signaling is believed to be the key factor in the satiety-deficient eating evident in the OBZ rats. We found that fat infiltration into the tongue muscle in OBZ rats was significantly greater than in the masseter muscle and skeletal upper airway muscle in OBZ rats. The difference in tongue fat compared to the fat in the masseter muscle could be related to a difference in leptin expression/signaling in tongue or masseter muscle tissues, although there are no data to support such a difference. In addition, other possible mechanisms of increased fat deposition in the tongue would include an overall increase serum level of free fatty acid in OBZ rats[41] and possible alterations in the collagen extracellular matrix[42] (i.e., increase in the lipids not bound in cell membranes lipids).

Recent studies on diet-induced obesity in rats indicate that the propensity to gain weight is different among animals of the same strain and may be caused by molecular adaptations that involve neuropeptide and paracrine signaling differences among the same animal strains.[43] An experiment that might differentiate the effects of a leptin-receptor defect in genetically compromised (fa/fa) OBZ rats from environmentally susceptible obesity would be to perform the experimental protocols from this study on matched group of diet-induced obese rats.[43] These diet-induced obese rats could be studied in age-matched groups and compared among weight-matched groups across ages and at the same age as OBZ rats (in our study). In such an experiment, tongue fat infiltration could be examined in rats of the same strain having developed obesity because of diet-related changes rather than from a leptin defect.

Potential Effects of Tongue Fat on its Function

Gilbert et al.[44] describes the tongue as a hydrostat that conserves overall volume but changes shape as muscles contract. According to this model, the tongue is composed of orthogonally oriented fibers and its mechanical behavior (changing shape with constant volume) relies on high water content within the tongue that that is relatively mobile and can diffuse throughout the tongue as opposing fibers contract or relax.[44,45] If fat infiltration in the tongue is found to be heterogeneously distributed and interferes with the movement of water during contraction of muscle fibers, this could be detrimental to the mechanical action of the tongue.

Moreover, in a dynamic study of tongue shape and changes in obese and weight-matched patients with OSA, Brown et al.[46] found that patterns of tongue displacement during respiration were significantly different in obese patients. Obesity in general limited the degree to which the tongue could create a patent upper airway during respiration.[47] Thus, an increase in tongue fat infiltration with obesity may affect airway dynamics by altering the pattern of tongue displacement during respiration. Furthermore, evidence of connective tissue alterations with obesity[42] may be a factor in altering the way in which tongue fibers are able to change tongue shape or effectively displace the tongue (to increase upper airway patency) during respiration.

To our knowledge there have been no direct measurements of tongue tissue pressure but Kairaitis et al.[48] found that extracellular tissue pressure, i.e., in tissues surrounding the airway and the tongue, was lower with mandible advancement in rabbits. Winter et al.[49] also investigated pharyngeal tissue pressure and measured inspiratory-related decreases and expiratory-related increases in the fat pads in the pharynx of anesthetized pigs during breathing. They postulated that because of lower tissue density of fat (0.9 g/cm^3) compared to water or muscle, tissue pressure variations would be greater in the lateral fat pad tissues (compared to skeletal muscle tissue). Thus, the replacement of water or muscle with fat in the tongue might also cause a decrease in tongue stiffness. A study examining magnetic resonance elastography to measure the shear modulus (a measure of stiffness) of the tongue and pharyngeal tissues in normal human patients has been recently published.[50] Changes in tissue pressure, precise measurement of tissue motion, and the related biomechanical properties of airway tissues is an important future direction to understanding how obesity may alter overall upper airway mechanics.[47] Better understanding of the consequences of tongue fat accumulation could be examined in human or animal studies that examine tongue motion, with particular focus on the phasic and pattern changes that may result from contractile timing changes with obesity.[46,50,51]

In conclusion, we found an unequivocal increase in fat in the tongue in OBZ rats compared with NBZ rats. The infiltration of fat in the tongue with obesity was greater in proportion to the general increase of fat in other skeletal muscle. Our data suggest that future studies of the role of obesity in sleep apnea should focus on tongue fat and what are the determinants of this fat distribution. The significant fat increase and sequestration in the OBZ rat tongue may play a role in altered tongue neuromuscular function, tongue stiffness, and metabolic function.

ACKNOWLEDGMENTS

Author contributions: conception and design – Dr. Brennick, Dr. Pack, Dr. Pickup, Dr. Buxbaum, Ms. Roscoe, Dr. Delikatny, and Dr. Schwab; analysis and interpretation – Dr. Brennick, Dr. Pack, Dr. Pickup, Dr. Buxbaum, Dr. Roscoe, Mr. Kim, Dr. Cater, Dr. Delikatny, Dr. Zhu, Ms. Shinde, and Dr. Schwab; drafting the manuscript for important intellectual content – Dr. Brennick, Dr. Pack, Dr. Buxbaum, Dr. Cater, Dr. Delikatny, Dr. Zhu, and Dr. Schwab. The authors acknowledge the support staff of the Small Animal Imaging Facility, Department of Radiology, Pereleman School of Medicine, University of Pennsylvania, Philadelphia, PA. We also acknowledge the help of Elizabeth B. Kneeland and Dana Concio in the preparation of this manuscript.

DISCLOSURE STATEMENT

This was not an industry supported study. The study was supported by NIH grants: HL-094307 (to Dr. Pack), HL-077838 (to Dr. Brennick), HL-077838 (to Dr. Brennick), HL-089447 (to Dr. Schwab) and AI-081717 (to Dr. Buxbaum). Dr. Schwab has consulted for and received research support from ApniCure. The other authors have indicated no financial conflicts of interest.

REFERENCES

1. Foster GD. Principles and practices in the management of obesity. Am J Respir Crit Care Med 2003;168:274-80.

2. Hedley AA, Ogden CL, Johnson CL, Carroll MD, Curtin LR, Flegal KM. Prevalence of overweight and obesity among US children, adolescents, and adults, 1999-2002. JAMA 2004;291:2847-50.
3. Kuczmarski RJ, Carroll MD, Flegal KM, Troiano RP. Varying body mass index cutoff points to describe overweight prevalence among U.S. adults: NHANES III (1988 to 1994). Obes Res 1997;5:542-8.
4. Ogden CL, Carroll MD, Curtin LR, McDowell MA, Tabak CJ, Flegal KM. Prevalence of overweight and obesity in the United States. JAMA 2006;295:1549-55.
5. Ogden C, Carroll M, Kit B, Flegal K. Prevalence of obesity in the United States, 2009-2010. NCHS data brief, no 82. In: Statistics NCfH, ed. Hyattsville, MD, 2012.
6. Banno K, Walld R, Kryger MH. Increasing obesity trends in patients with sleep-disordered breathing referred to a sleep disorders center. J Clin Sleep Med 2005;1:364-6.
7. Newman AB, Foster G, Givelber R, Nieto FJ, Redline S, Young T. Progression and regression of sleep disordered breathing with changes in weight: The Sleep Health Study. Arch Intern Med 2005;165:2408-13.
8. Schwab RJ, Kuna ST, Remmers JE. Anatomy and physiology of upper airway obstruction. In: Kryger, Roth, Dement, eds. Principles and practice of sleep medicine, 4th ed. Philadelphia: W.B. Saunders, 2005:840-58.
9. Hausman DB, Fine JB, Tagra K, Fleming SS, Martin RJ, DiGirolamo M. Regional fat pad growth and cellularity in obese Zucker rats: modulation by caloric restriction. Obes Res 2003;11:674-82.
10. Nashi N, Kang S, Barkdull GC, Lucas J, Davidson TM. Lingual fat at autopsy. Laryngoscope 2007;117:1467-73.
11. Schwab RJ, Pairstein M, Kaplan L, et al. Family aggregation of upper airway soft tissue structures in normal subjects and patients with sleep apnea. Am J Respir Crit Care Med 2006;173:453-63.
12. Schwab RJ, Pairstein M, Pierson R, et al. Identification of upper airway anatomic risk factors for obstructive sleep apnea with volumetric magnetic resonance imaging. Am J Respir Crit Care Med 2003;168:522-30.
13. Kim A, Keenan B, Jackson N, et al. Tongue fat and its relationship to obstructive sleep apnea. Sleep 2014 (in press).
14. Boyd JH, Petrof BJ, Hamid Q, Fraser R, Kimoff RJ. Upper airway muscle inflammation and denervation changes in obstructive sleep apnea. Am J Respir Crit Care Med 2004;170:541-6.
15. Stauffer JL, Buick MK, Bixler EO, et al. Morphology of the uvula in obstructive sleep apnea. Am Rev Respir Dis 1989;140:724-8.
16. Zohar Y, Sabo R, Strauss M, Schwartz A, Gal R, Oksenberg A. Oropharyngeal fatty infiltration in obstructive sleep apnea patients: a histologic study. Ann Otol Rhinol Laryngol 1998;107:170-4.
17. Strobel K, Hoff Jvd, Pietzsch J. Localized proton magnetic resonance spectroscopy of lipids in adipose tissue at high spatial resolution in mice in vivo. J Lipid Res 2008;49:473-80.
18. Dong Z, Hwang JH. Lipid signal extraction by SLIM: application to 1H MR spectroscopic imaging of human calf muscles. Magn Reson Med 2006;55:1447-53.
19. Brennick MJ, Pack AI, Ko K, et al. Altered upper airway and soft tissue structures in the New Zealand obese mouse. Am J Respir Crit Care Med 2009;179:158-69.
20. Glover GH, Schneider E. Three-point Dixon technique for true water/fat decomposition with B0 inhomogeneity correction. Magn Reson Med 1991;18:371-83.
21. Folch J, Lees M, Sloane Stanley GH. A simple method for the isolation and purification of total lipides from animal tissues. J Biol Chem 1957;226:497-509.
22. De Bock K, Dresselaers T, Kiens B, Richter EA, Van Hecke P, Hespel P. Evaluation of intramyocellular lipid breakdown during exercise by biochemical assay, NMR spectroscopy, and Oil Red O staining. Am J Physiol Endocrinol Metab 2007;293:E428-34.
23. Farkas GA, Schlenker EH. Pulmonary ventilation and mechanics in morbidly obese Zucker rats. Am J Respir Crit Care Med 1994;150:356-62.
24. Brennick MJ, Pickup S, Cater JC, Kuna ST. Phasic respiratory pharyngeal mechanics by magnetic resonance imaging in lean and obese Zucker rats. Am J Respir Crit Care Med 2006;173:1031-7.
25. Nakano H, Magalang UJ, Lee S-d, Krasney JA, Farkas GA. Serotonergic modulation of ventilation and upper airway stability in obese Zucker rats. Am J Respir Crit Care Med 2001;163:1191-7.
26. Brennick MJ, Shinde SA, Kim DH, Delikatny EJ, Schwab RJ. Increased tongue muscle fat in obese vs. lean Zucker rats by in-vivo magnetic resonance spectroscopy. Am J Respir Crit Care Med 2011;183:A3680.
27. Shinde S, Brennick MJ, Bearn CB, Delikatny J, Schwab RJ. Fat infiltration in the tongue of obese versus lean Zucker rats. Am J Respir Crit Care Med 2013;187:A5470.
28. Argmann CA, Houten SM, Champy M-F, Auwerx J. Lipid and Bile Acid Analysis. Current Protocols in Molecular Biology. Hoboken: John Wiley & Sons, Inc., 2006:2-24.
29. Goodpaster B, Theriault R, Watkins S, Kelley D. Intramuscular lipid content is increased in obesity and decreased by weight loss. Metabolism 2000;49:467-72.
30. Westfall PH, Tobias RD, Rom D, Wolfinger RD, Hochberg Y. Multiple Comparisons and Multiple Tests Using the SAS System. 1 ed. Cary: SAS Institute, Inc., 1999.
31. Hayter AJ. Pairwise comparisons of genreally correlated means. J Am Statist Assoc 1989;84:208-13.
32. Ross R, Leger L, Guardo R, De Guise J, Pike BG. Adipose tissue volume measured by magnetic resonance imaging and computerized tomography in rats. J Appl Physiol (1985) 1991;70:2164-72.
33. Folch J, Ascoli I, Lees M, Meath JA, LeBaron N. Preparation of lipide extracts from brain tissue. J Biol Chem 1951;191:833-41.
34. Brennick MJ, Kuna ST, Pickup S, Cater J, Schwab RJ. Respiratory modulation of the pharyngeal airway in lean and obese mice. Respir Physiol Neurobiol 2011;175:296-302.
35. Fuller D, Mateika JH, Fregosi RF. Co-activation of tongue protrudor and retractor muscles during chemoreceptor stimulation in the rat. J Physiol 1998;507:265-76.
36. Magalang UJ, Ray AD, Farkas GA. Effects of hypoglossal nerve stimulation on upper airway mechanics in obese Zucker rats. Am J Respir Crit Care Med 2002;165:A798.
37. Polotsky M, Elsayed-Ahmed AS, Pichard L, et al. Effect of age and weight on upper airway function in a mouse model. J Appl Physiol. 2011;111:696-703.
38. Fuller DD, Williams PL, Janssen PL, Fregosi RF. Effect of co-activation of tongue protrudor and retractor muscles on tongue movements and pharyngeal airflow mechanics in the rat. J Physiol 1999;519:601-13.
39. Magalang UJ, Farkas GA, Najdzionek JS, Nakano H. Obese Zucker rats have narrower upper airway compared to lean litter-mates [abstract]. Am J Respir Crit Care Med 2000;161:A87.
40. Schaser A, Wang H, Volz LM, Connor CP. Biochemistry of the anterior, medial and posterior genioglossus in the aged rat. Dysphagia 2011;26:256-63.
41. Oakes ND, Kjellstedt A, Thalen P, Ljung B, Turner N. Roles of fatty acid oversupply and impaired oxidation in lipid accumulation in tissues of obese rats. J Lipids 2013;2013:420754.
42. Dantas DA, Mauad T, Silva LF, Lorenzi-Filho G, Formigon GG, Cahali MB. The extracellular matrix of the lateral pharyngeal wall in obstructive sleep apnea. Sleep 2012;35:483-90.
43. Tulipano G, Vergoni AV, Soldi D, Muller EE, Cocchi D. Characterization of the resistance to the anorectic and endocrine effects of leptin in obesity-prone and obesity-resistant rats fed a high-fat diet. J Endocrinol 2004;183:289-98.
44. Gilbert RJ, Napadow VJ, Gaige TA, Wedeen VJ. Anatomical basis of lingual hydrostatic deformation. J Exp Biol 2007;210:4069-82.
45. Napadow VJ, Chen Q, Wedeen VJ, Gilbert RJ. Intramural mechanics of the human tongue in association with physiological deformations. J Biomech 1999;32:1-12.
46. Brown EC, Cheng S, McKenzie DK, Butler JE, Gandevia SC, Bilston LE. Respiratory movement of upper airway tissue in obstructive sleep apnea. Sleep 2013;36:1069-76.
47. Brennick MJ. Understanding airway tissue mechanics is a step towards improving treatments in OSA. Sleep 2013;36:973-4.
48. Kairaitis K, Stavrinou R, Parikh R, Wheatley JR, Amis TC. Mandibular advancement decreases pressures in the tissues surrounding the upper airway in rabbits. J Appl Physiol 2006;100:349-56.
49. Winter WC, Gampper T, Gay SB, Suratt PM. Lateral pharyngeal fat pad pressure during breathing in anesthetized pigs. J Appl Physiol 1997;83:688-94.
50. Cheng S, Gandevia SC, Green M, Sinkus R, Bilston LE. Viscoelastic properties of the tongue and soft palate using MR elastography. J Biomech 2011;44:450-4.
51. Cheng S, Butler JE, Gandevia SC, Bilston LE. Movement of the tongue during normal breathing in awake healthy humans. J Physiol 2008;586:4283-94.

MRS Acquisition and Analysis

Anesthetic induction was performed in a Plexiglas® box as rats breathed 3% isoflurane (v/v) in 100% oxygen (approximately 5 minutes) until the withdrawal reflex was absent. Rats were placed supine on a custom platform inside the MRI coil and breathed spontaneously through a nose cone (2%-3% isoflurane in O_2) with body temperature maintained at 36-37°C with a water-heating pad. A monitoring system (Small Animal Instruments, Stony Brook, NY) measured core body temperature, and a compliant pressure sensor positioned over the diaphragm measured respiratory rate and generated a trigger signal at end-inspiration to allow MRI (and MRS) gating to the expiratory phase to minimize motion artifact.

MRS data were processed using Mac Nuts® (AcornNMR.com) software with built-in algorithms to employ a 1 Hz line broadening, Fourier transformation, manual zeroing (of the water peak), first order phase correction and baseline (background noise) correction. From the processed spectra, the areas under the lipid and water peaks were determined by integration of the best-fit polynomial (computer-generated) equations fitted to those peaks. The lipid peak was assumed to be at 1.3 ppm in the adjusted spectrum where the center of the water peak was set to 4.7 ppm that is the known standard for this 4.7T, 200MHz system[1] (see Figure 2 in the manuscript). Comparison of the lipid content between animals was determined taking the ratio of the area of the lipid peak in water suppressed spectra, to the area of the water peak of the same voxel from the spectra acquired without water suppression (see Figure 2 in the manuscript). Thus, in a specific voxel, the signal from the water peak using the same gain and acquisition variables in all spectra, was used to normalize the signal of interest in the lipid peak obtained with water suppression in that specific voxel.

Determination of the dimensionless lipid-to-water ratio involved the manual zeroing of the water peak, phase correction and background noise correction. The lipid-to-water ratio was determined in three trials for each voxel in the tongue and masseter muscle and the averaged the three trials were used. In some cases, particularly in the masseter muscle, there was lower signal-to-noise compared to most tongue spectra thus the lipid peak could not always be distinguished or measured in the water-suppressed H^1 spectra using MacNuts processing. Thus, a reduced number of animals' MRS lipid content were compared in the masseter of NBZ and OBZ rats.

Tongue Volume and Tongue Fat by MRI: Image Acquisition and Analysis

On the same day or within 2-3 days subsequent to the MRS experiment, a Dixon 3-pt. protocol,[2] during the (gated) expiratory phase of breathing, was used to obtain axial slices that encompassed the tongue in the rat upper airway. The gated acquisition reduced the level of motion artifact and use of the expiratory phase allowed for adequate acquisition time needed for the spin-echo sequence. Thirteen, 2.0 mm thick axial slices, field of view 50 × 50 mm, were planned from a mid-sagittal scout image of the rat head to encompass the entire tongue from anterior tip to just below the base of the tongue, using the larynx as a caudal landmark. The Dixon 3-point protocol,[2] modified for use on the Varian console, utilized a spin-echo sequence at two resonance points, that of water and one obtained from the midpoint of the fat peak frequency offset (after shimming, usually 600-700 nm to the right of the peak water resonance on the 200 MHz imaging system). The Dixon spin-echo acquisition parameters were: excitation time (TE) = 15 ms, repetition time (TR) for all slices = the expiration time (range from 600 to 800 ms), with a 128 square pixel matrix (nominal resolution = 0.39 mm/pixel in the axial plane, 2.0 mm between slices).

Tongue volume and tongue fat were determined in each rat using an analysis protocol that first aligned the contiguous set of axial image slices in each rat to a single 'registration slice' i.e., the caudal axial slice where bilateral tympanic bulla appear as dark round holes lateral to the pharyngeal airway.[3] Thus, there were six (6), 2 mm thick MRI axial slices of the posterior region of the tongue, ventral to the soft palate, and seven (7), 2 mm thick MRI slices encompassing the mid-to-anterior tongue (anterior to the junction of the soft to hard palate, ventral to the hard palate) that formed two regions of the tongue denoted as posterior and anterior.

The proton weighted images were analyzed with manual segmentation of the tongue muscle in each axial slice.[4,5] Once the boundaries of the tongue were obtained, computer overlay (Amira, VSG, Burlington, MA) of the tongue segments were identified on the fat-discriminated images. Total fat (mm^3) in the tongue portion of the Dixon fat-weighted images was determined using by a threshold method described below.

The fat-weighted images were displayed using Amira software on a 0-254 scale (with 2 bytes reserved for masking). The fat-weighted images were not strictly black or white but showed a gradient of white to gray to black intensities due to the relative concentration of fat in the image. Each series of axial images was analyzed using a threshold method to differentiate the fat-weighted signal from the surrounding tissues (where there was little or no fat-weighted signal). First, the minimum and maximum signal strength of fat in the image were determined by changing the image intensity value while observing: (1) when the oil phantom standard was brightest (maximum value), and (2) when the oil phantom intensity disappeared (minimum value). In some cases, where the phantom was not adequately imaged, the subcutaneous fat of the rat was used as the standard to obtain the threshold values. Second, since individual images and series reflected a varying degree of background noise we added to the minimum threshold value a noise correction value. This value, considered an estimate of the noise in the image[6] was determined from the standard deviation of the mean pixel values measured from a region of the black space at the outer boundary of the image. Thus, by this threshold method, similar to that in our previous study[7] fat volume (mm^3) was considered the sum of pixels in the range above the lowest black space intensity and below the highest white color intensity, as measured from the oil-phantom (assumed highest lipid content-intensity) in the axial images.

Biochemical Methods and Analysis

Following the MRS and MRI experiments the rats were euthanized by CO_2 insufflation. The tongue was surgically removed by cutting the ventral mucosal tissues in the oral sulcus adjacent to the tongue followed by bilateral section of the mandible at the temporal bony attachment. The tongue accessory muscles: geniohyoid, hyoglossus and styloglossus were blunt dissected along membranous tissue boundaries from the tongue and the tongue was further dissected from all attachments to the basohyoid bone. Thus, the extracted postmortem tongues (mean weights, Table 3) were free of the large hypoglossal nerve branches, sublingual arteries and extrinsic muscles except the genioglossus muscle. A tissue sample, approximately 3 mm^3, of the masseter muscle, was also dissected during the postmortem rat dissections. The tissue extracts were quick frozen in dry ice then stored at -82 C until further analysis. To conserve tissue for possible re-analysis, we divided each tongue on its long axis (anterior to posterior length) into two equal symmetrical parts. This provided approximately 0.5 g tongue tissue for biochemical analysis that was the ideal tissue quantity, from which preliminary results in trial samples showed reasonable and repeatable colorimetric results.

The Folch method of lipid purification for animal tissue extracts was used to assess the lipid or triglyceride (fat) content in the muscle tissue of the tongue and masseter muscles.[8,9] In brief, we homogenized 500 mg of tissue with 0.9 ml chloroform : methanol (2:1) mixture in a Gerresheimer tissue grinder, followed by the addition of 0.3 ml methanol to decrease specific gravity. Samples were centrifuged at 750g for 15 min to remove insoluble material. 400 µl chloroform and 275 µl 0.73% NaCl were added to the supernatants and vortexed 30 sec. The resulting mixture separated into two phases, where the lower chloroform/methanol-rich phase contained triglycerides. The salts alter the distribution of lipids and drive them from the upper aqueous phase. The Folch separation of the tongue (or masseter) muscle samples produced a lipid extract from which the triglyceride content of rat's tongue was determined using Enzymatic-Colorimetric Triglyceride Kit (Standby Triglyceride Liquid Color Procedure No.2200; Stanbio, Boeme, TX).

Enzymatic assays were performed using 20 µl of sample and standards in a 96-well microtiter plate. Using two-fold serial dilution for both standard and sample in triplicate, concentrations of 3.125 - 200 mg/dl of the standard were generated. Color was developed on the triglyceride plate by adding 180 µl of reagent to 20 µl of sample, allowing this mixture to stand 10 min before reading. Glycerol and fatty acids are first formed by lipase action on the triglycerides, and glycerol is converted to the color product through the process of an enzymatic reaction. Plates were read on a Bio-Rad- Model 680 Microplate Reader and data analyzed using MicroPlateManager III 1.80 (Bio-Rad, Hercules, CA) at 490 nm wavelength. From the linear standard curve the results were calculated as total triglyceride concentration and converted into milligram triglyceride per gram of tissue.

In order to assure consistency of results the triplicate values were statistically compared in each run to obtain the coefficient of variance among them and only values that were below a limit of 15% variance were used. In most cases coefficient of variance values were well under 10% indicating repeatability and confidence in the triplicate colorimetry measurements. In addition, the lipid standard from which the calibration dilutions were created in each assay, was obtained at 200 mg/dl in a single bulk solution so that all assays came from the same source of standard lipid solution.

Histological Methods

Quantitative measures of triglyceride (lipid content) were provided in the biochemistry, Dixon fat discriminated MR image analysis and in semi-quantitative (non-dimensional) MR spectroscopy analysis. The histological protocol was designed to provide qualitative information to assess and compare fat distribution in the OBZ and NBZ tongues i.e., homogenous or regional distribution, and reveal the degree of fat infiltration within or outside muscle cells. Oil Red O staining[10,11] was used with hematoxylin counter stain. Two each of OBZ and NBZ tongues were set aside for histological analysis.

Briefly, postmortem tongues dissected as described above, were cut along the sagittal mid-line in equal halves and embedded in Tissue-Tek embedding medium (Sakura Finetek Inc. Torrance, CA) on dry ice then stored at –80°C. Cryostat sagittal sections (10 µm) were collected in series, stored at –80°C, followed later by Oil Red Oand hematoxylin counter- staining.

The "Oil Red O" (ORO) staining protocol was performed according to the IHC world protocols (IHCworld.com, http://www.ihcworld.com/_protocols/special_stains/oil_red_o.htm). Tissue sections were fixed with cold 4% Para formaldehyde for 10 min on ice then washed with distilled water. The sections were stained in pre-warmed 0.5% ORO solution for 10 min at 60°C, followed by differentiation in 85% propylene glycol solution for 3 min. The ORO solution was prepared by using 500mg ORO (A12989, CAS#1320-06-5, Alfa Aesar, Ward Hill, MA) dissolved in 100ml propylene glycol at 95°C then filtered to remove crystallized ORO. After washing with distilled water, the sections were counterstained using Hematoxylin Stain Solution (CS400-1D, Fisher Scientific, Pittsburgh, PA) for 3 min. to visualize nuclei. The sections were then gently rinsed with tap water and covered with a cover slip using glycerin jelly mounting medium (http://www.ihcworld.com/_protocols/histology/mounting_medium.htm).

Imaging was performed with a Leica system at 10X- 400X (DM5500B scope, DFC425 camera and AF6000 software, Leica Microsystems Inc, Buffalo Grove, IL). The sections also were imaged using a Leica TCS SP-5 confocal microscope to get high magnification pictures. Oil Red O stained sections were examined with the emission wavelength at Leica/ALEXA 594. A combination, differential interference contrast image was obtained by combining a non-confocal image, collected simultaneously with a confocal image.

Statistical Methods

A mixed model ANOVA was used on each sub method section i.e., MRS, biochemistry and MRI analyses.[12] In all cases, for main effects and Tukey adjusted pos-hoc contrasts, significance was assumed at $P < 0.05$.[13] In the MRS and biochemistry analyses, differences in the ages or body weights of OBZ or NBZ rats were tested. Since MRI data were acquired on the same or within 2-3 days as MRS data explicit age and weight

comparisons on this sub-group were assumed not to be different than those of the MRS data set.

Specifically, in MRS, the lipid-to-water ratio of voxels of the tongue were compared between OBZ and NBZ groups. Tukey post-hoc procedure tested differences within tongue regions: posterior, mid-rostral level or total tongue (averaged in each animal) results and between regions in OBZ and NBZ rats. Masseter muscle lipid-to-water ratios from MRS in a data set with smaller n, were compared separately (using one-way ANOVA) between OBZ and NBZ rat groups. One-way ANOVA was also used to determine whether lipid-to-water ratios in the masseter were different than those in NBZ and OBZ the tongue muscle.

MRI volumetric analyses tested whether OBZ and NBZ rats had different tongue volumes using a mixed model ANOVA. Tissue volume, and separately Dixon protocol fat content were compared between OBZ and NBZ rats and among regional tongue volumes (posterior, anterior or total tongue).

The biochemistry statistical analysis was similar to that used in the MRS analysis that included the mixed model ANOVA to test animal weights and ages (used in this sub-component) between OBZ and NBZ rat types. The variable tested was the calculated triglyceride tissue concentration in mg/g, i.e. milligram triglyceride per gram tongue tissue or per gram masseter muscle tissue. Additionally, the mixed model ANOVA analysis for the biochemical results tested whether masseter muscle triglyceride concentration was different than triglyceride concentration in the tongue muscle (for OBZ and NBZ rats) thus whether obesity altered the masseter triglyceride tissue concentration.

REFERENCES

1. Strobel K, Hoff Jvd, Pietzsch J. Localized proton magnetic resonance spectroscopy of lipids in adipose tissue at high spatial resolution in mice in vivo. J Lipid Res 2008;49:473-80.
2. Glover GH, Schneider E. Three-point Dixon technique for true water/fat decomposition with b inhomogeneity correction. Magn Reson Med 1991;18:371-83.
3. Brennick MJ, Pickup S, Cater JC, Kuna ST. Phasic respiratory pharyngeal mechanics by magnetic resonance imaging in lean and obese Zucker rats. Am J Respir Crit Care Med 2006;173:1031-7.
4. Hebel R, Stromberg MW. In: Hebel R, Stromberg MW (Hrsg) Anatomy and embryology of the laboratory rat; BioMed Verlag, Wörthersee 1986.
5. Hayakawa T. A color atlas of sectional anatomy of the rat. International ed. Tokyo: Adosuri: Marusen (hatsubai), 2008.
6. McGibney G, Smith MR. An unbiased signal to noise ratio measurement for magnetic resonance images. Med Phys 1993;20:1077-8.
7. Schwab RJ, Pasirstein M, Pierson R, et al. Identification of upper airway anatomic risk factors for obstructive sleep apnea with volumetric magnetic resonance imaging. Am J Respir Crit Care Med 2003;168:522-30.
8. Argmann CA, Houten SM, Champy M-F, Auwerx J. Lipid and Bile Acid Analysis. Current Protocols in Molecular Biology: John Wiley & Sons, Inc., 2006:2-24.
9. Folch J, M.Lees, Stanley GHS. A simple method for the isolation and purification of total lipides from animal tissues. J Biol Chem 1956;226:497-509.
10. Bock KD, Dresselaers T, Kiens B, Richter EA, Hecke PV, Hespel P. Evaluation of intramyocellular lipid breakdown during exercise by biochemical assay, NMR spectroscopy, and Oil Red O staining. Am J Physiol Endocrinol Metab 2007;293:E428-E34.
11. Goodpaster B, Theriault R, Watkins S, Kelley D. Intramuscular lipid content is increased in obesity and decreased by weight loss. Metabolism 2000;49:467-72.
12. Westfall PH, Tobias RD, Rom D, Wolfinger RD, Hochberg Y. Multiple Comparisons and Multiple Tests Using the SAS System. 1 ed. Cary: SAS Institute, Inc., 1999.
13. Hayter AJ. Pairwise comparisons of genreally correlated means. J Am Stat Assoc 1989;84:208-13.